Synthesis and Structural Features of New Ruthenium(II) Complexes Containing the Scorpionate Ligands Tris(pyrazol-1-yl)methanesulfonate (Tpms) and Tris(pyrazol-1-yl)methane (Tpm)

Sara Miguel,[a] Josefina Diez,[a] Mª Pilar Gamasa,[a] and Mª Elena Lastra*[a]

Keywords: Ruthenium / Scorpionate ligands / Phosphane ligands / N,O ligands

New ruthenium(II) scorpionate complexes containing tris-(pyrazol-1-yl)methanesulfonate (Tpms) and tris(pyrazol-1-yl)-methane (Tpm) ligands have been synthesized. For complexes with Tpms, two isomers are obtained as the kinetic (**1a**) and thermodynamic (**1b**) products, which shows that, for these complexes, the $\kappa^3(N,N,N)$ coordination mode of the Tpms ligand is favored over $\kappa^3(N,N,O)$ coordination. In addition, complexes with water soluble phosphane ligands 1,3,5-triaza-7-phosphatricyclo[3.3.1.1^{3,7}]decane (PTA) and 1-alkyl-3,5-diaza-1-azonia-7-phosphatricyclo[3.3.1.1^{3,7}]decane (1-R-PTA) have been prepared and structurally characterized.

Introduction

Scorpionate ligands have been widely used in coordination chemistry due to the rich chemistry of their metal complexes, which have been extensively used in stoichiometric and catalytic chemistry. In particular, complexes bearing the anionic tris(pyrazol-1-yl)borate (Tp) ligand have been prominently studied.[1] However, the chemistry of transition metal complexes bearing other trispyrazolyl ligands has been far less developed.

For instance, tris(pyrazolyl)alkanes, such as tris(pyrazol-1-yl)methane (Tpm), constitute a family of stable and flexible polydentate ligands isoelectronic and isosteric with tris(pyrazolyl)borates, the major difference being the charge.[2] Replacement of the methyne proton in Tpm by a methanesulfonate unit[3] leads to the tris(pyrazol-1-yl)methanesulfonate ligand (Tpms). This ligand constitutes a versatile alternative to tris(pyrazolyl)borate, as the sulfonate group is noninnocent and plays a determining role on the properties of the complexes, for example by imparting hydrosolubility.

In addition, the oxygen atom from the sulfonate unit may coordinate with the metal atoms. Thus, for this ligand, apart from the tripodal $\kappa^3(N,N,N)$ coordination mode,[4] $\kappa^3(N,N,O)$ coordination has been described for several metal complexes,[5] which can be used as models for N,N,O binding in metalloenzymes,[6] regardless that the sulfonate unit is a weakly coordinating group, especially in comparison with nitrogen atom donors. Moreover, $\kappa^2(N,N)$ coordination of Tpms has been described for rhodium(I) complexes[7] and proposed for iridium(I) catalysts.[8]

This versatile behavior of the Tpms ligand and the increased water solubility of its complexes compared to Tp complexes, prompted us to explore the chemistry of ruthenium complexes as, to the best of our knowledge, no ruthenium complexes have been synthesized with this ligand.

We have recently reported the synthesis and antitumor activity of a series of ruthenium(II) complexes containing tris(pyrazol-1-yl)borate.[9] In this article, we report the synthesis and structural features of ruthenium(II) complexes bearing the scorpionate ligand Tpms (Figure 1). Furthermore, our interest in water soluble complexes, which could be used in biological assays, prompted us to study phosphane substitution with the water soluble 1,3,5-triaza-7-phosphatricyclo[3.3.1.1^{3,7}]decane (PTA) phosphane as well as electrophilic attacks on coordinated PTA phosphanes yielding new ruthenium(II) complexes. Synthesis and reactivity studies of the cationic complex [RuCl{$\kappa^3(N,N,N)$-Tpm}(PPh$_3$)(PTA)]Cl, bearing neutral Tpm, are also described.
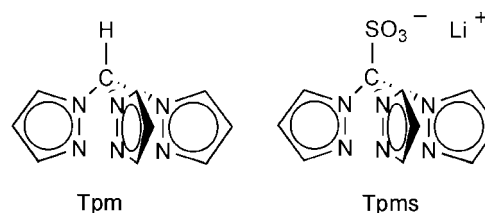
[a] Departamento de Química Orgánica e Inorgánica, Instituto de Química Organometálica "Enrique Moles" (Unidad Asociada al C.S.I.C.), Universidad de Oviedo, 33006 Oviedo, Principado de Asturias, Spain Fax: +34-985103446 E-mail: elb@uniovi.es

Figure 1. Tpm and Tpms ligands.

Results and Discussion

Ruthenium(II) Complexes Containing $\kappa^3(N,N,N)$- and $\kappa^3(N,N,O)$-Tpms. Synthesis of [RuCl{$\kappa^3(N,N,N)$-Tpms}(PPh₃)₂] (1a) and [RuCl{$\kappa^3(N,N,O)$-Tpms}(PPh₃)₂] (1b)

The reaction of one equivalent of the lithium salt of Tpms with [RuCl₂(PPh₃)₃] in hot methanol gave [RuCl{$\kappa^3(N,N,N)$-Tpms}(PPh₃)₂] (**1a**), which was isolated as a yellow solid in 95% yield. When this reaction was carried out in a 1:10 CH₂Cl₂/MeOH mixture at 0 °C, [RuCl{$\kappa^3(N,N,O)$-Tpms}(PPh₃)₂] (**1b**) was isolated as an orange solid in 57% yield. When complex **1b** was heated in CH₂Cl₂, isomerization to **1a** was observed (Scheme 1), which indicates that **1a** is the thermodynamically stable product. Complete transformation can also be observed at room temperature within a few days.
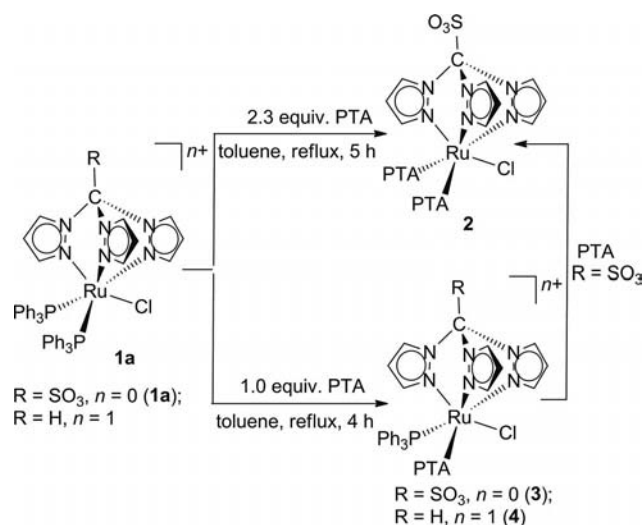
Scheme 1.

Spectroscopic data (IR and ¹H, ¹³C{¹H}, and ³¹P{¹H} NMR spectroscopy) support the proposed formulation. In particular, IR spectra are especially informative as they allow the establishment of the coordination mode of Tpms in the complexes. Thus, for **1a** the IR spectrum shows two medium signals at 1286 and 1054 cm⁻¹ due to the S–O bond and a weak band at 832 cm⁻¹ due to the C–N bond of the pyrazole rings. However, for **1b**, the IR spectrum shows more bands in the region 1400–1000 cm⁻¹ than for **1a**, and two different bands at 1088 and 860 cm⁻¹ for the C–N bonds can be observed, which indicate $\kappa^3(N,N,O)$ coordination for Tpms.[10] In both complexes, the band due to the C–S stretching vibration appears at 621 cm⁻¹.

The rest of the data are in accordance with the proposed structures: (i) a singlet resonance is observed at 38.9 (**1a**) and 35.8 (**1b**) ppm in the ³¹P{¹H} NMR spectra indicating the equivalence of the two phosphorus atoms for both complexes. For complex **1b**, this involves the oxygen atom from the methanesulfonate unit *trans* to the chlorine atom, (ii) the ¹H NMR spectrum of **1a** shows the signals for the hydrogen atoms of the pyrazole rings *trans* to the phos-

phanes as two doublets at 8.91 and 6.99 ppm (3-H and 5-H) and a triplet at 5.85 ppm (4-H) and the hydrogen atoms for the ring *trans* to the chloride as two doublets at 9.10 and 5.21 ppm (3-H and 5-H) and a triplet at 5.42 ppm (4-H). For **1b** the hydrogen atoms of the pyrazole rings *trans* to the phosphanes appear as two doublets at 6.99 and 6.97 ppm (3-H and 5-H) and a triplet at 5.79 ppm (4-H). The hydrogen atoms for the noncoordinated pyrazole ring appear at lower field as two doublets at 9.00 and 7.90 ppm (3-H and 5-H) and a triplet at 6.60 ppm (4-H), and (iii) ¹³C{¹H} NMR spectra show the expected signals for the two complexes. In all cases the assignment of the signals has been confirmed by 2D COSY, heteronuclear single quantum coherence (HSQC), and HMBC NMR experiments.

In order to determine the structural differences between **1a** and **1b**, X-ray diffraction studies were carried out. Slow diffusion of hexane into a solution of **1a** in dichloromethane or **1b** in tetrahydrofuran (THF), resulted in crystals of **1a**·CH₂Cl₂ and **1b**·THF suitable for X-ray diffraction studies. An ORTEP view of the molecules is shown in Figure 2, and selected bond lengths and angles are presented in Table 1.
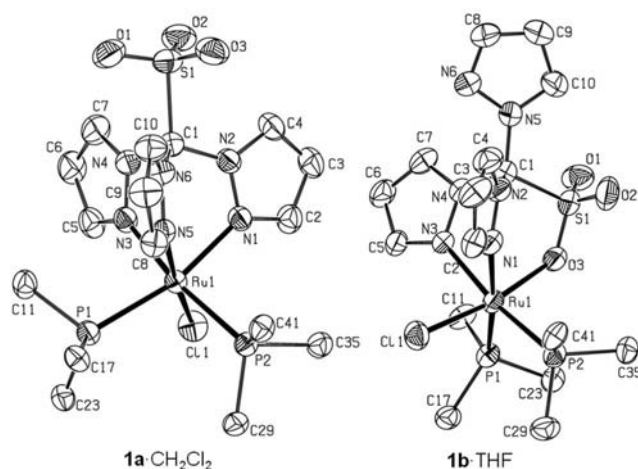

Figure 2. Molecular structure and atom labeling scheme for **1a**·CH₂Cl₂ and **1b**·THF. Solvent molecules and hydrogen atoms have been omitted for clarity. Non-hydrogen atoms are represented by 50% probability ellipsoids.

In both complexes, the ruthenium ion exhibits a distorted octahedral coordination geometry bonded to one chlorine atom, two phosphorus atoms of the PPh₃ ligands, and the Tpms ligand, which shows $\kappa^3(N,N,N)$ coordination for **1a** and $\kappa^3(N,N,O)$ coordination for **1b**. In **1b**, the chlorine atom is located *trans* to the oxygen atom and the third pyrazolyl ring acts a pendant uncoordinated pyrazolate group. $\kappa^3(N,N,O)$ coordination for Tpms has been described for several metal complexes.[5,6] Studies carried out with sterically hindered substituted Tpms point out that the ligand tends to adapt its coordination mode to suit the electronic and steric preferences of the metal center.[11]

The N–Ru–N angles and Ru–N bond lengths for both complexes are in the range found for hydridotris(pyrazolyl)-

Table 1. Selected bond lengths [Å] and angles [°] for **1a**·CH$_2$Cl$_2$ and **1b**·THF.

Selected bond lengths for **1a**·CH$_2$Cl$_2$			
Ru(1)–N(1)	2.128(2)	Ru(1)–P(1)	2.4002(7)
Ru(1)–N(3)	2.104(2)	Ru(1)–P(2)	2.3607(7)
Ru(1)–N(5)	2.068(2)	Ru(1)–Cl(1)	2.4060(7)

Selected bond angles for **1a**·CH$_2$Cl$_2$			
N(1)–Ru(1)–N(3)	79.07(9)	N(5)–Ru(1)–P(1)	88.73(7)
N(1)–Ru(1)–N(5)	84.10(9)	N(5)–Ru(1)–P(2)	96.56(6)
N(3)–Ru(1)–N(5)	87.06(10)	N(1)–Ru(1)–Cl(1)	88.81(7)
N(1)–Ru(1)–P(1)	166.29(7)	N(3)–Ru(1)–Cl(1)	86.92(7)
N(1)–Ru(1)–P(2)	91.66(6)	N(5)–Ru(1)–Cl(1)	171.46(7)
N(3)–Ru(1)–P(1)	88.92(7)	P(1)–Ru(1)–P(2)	100.78(2)
N(3)–Ru(1)–P(2)	169.68(7)	P(1)–Ru(1)–Cl(1)	97.22(3)
		P(2)–Ru(1)–Cl(1)	88.37(3)

Selected bond lengths for **1b**·THF			
Ru(1)–N(1)	2.135(5)	Ru(1)–P(1)	2.3683(17)
Ru(1)–N(3)	2.128(4)	Ru(1)–P(2)	2.3544(13)
Ru(1)–O(3)	2.131(4)	Ru(1)–Cl(1)	2.3917(15)

| Selected bond angles for **1b**·THF			
N(1)–Ru(1)–N(3)	77.15(18)	N(3)–Ru(1)–P(1)	92.25(14)
N(1)–Ru(1)–O(3)	90.40(18)	N(3)–Ru(1)–P(2)	169.76(13)
N(3)–Ru(1)–O(3)	83.64(15)	N(1)–Ru(1)–Cl(1)	83.25(14)
N(1)–Ru(1)–P(1)	169.26(12)	N(3)–Ru(1)–Cl(1)	87.92(12)
N(1)–Ru(1)–P(2)	93.47(12)	O(3)–Ru(1)–Cl(1)	170.40(11)
O(3)–Ru(1)–P(1)	86.63(12)	P(1)–Ru(1)–P(2)	96.97(5)
O(3)–Ru(1)–P(2)	92.43(10)	P(1)–Ru(1)–Cl(1)	98.29(6)
		P(2)–Ru(1)–Cl(1)	95.12(5)

borate ruthenium(II) complexes. N–Ru–N bond angles for **1a**·CH$_2$Cl$_2$ (79.07–87.06°) are larger than that for **1b** (77.16°) and close to the N–Ru–O bond angles (83.65–90.29°). For **1a**, the shortest Ru–N bond length corresponds to Ru(1)–N(5) [2.068(2) Å], which is *trans* to the chlorine atom, in accordance with the higher *trans* influence of the phosphane ligands.[12]

Complexes with PTA – Synthesis of [RuCl{κ^3(*N,N,N*)-Tpms}(PTA)$_2$] (2), [RuCl{κ^3(*N,N,N*)-Tpms}(PPh$_3$)(PTA)] (3), and [RuCl{κ^3(*N,N,N*)-Tpm}(PPh$_3$)(PTA)][Cl] (4)

Complex **1a** underwent phosphane substitution with PTA under different reaction conditions, which led to [RuCl{κ^3(*N,N,N*)-Tpms}(PTA)$_2$] (**2**) and [RuCl{κ^3(*N,N,N*)-Tpms}(PPh$_3$)(PTA)] (**3**). In order to establish a comparison between complexes with Tpms and Tpm, analogous [RuCl{κ^3(*N,N,N*)-Tpm}(PPh$_3$)(PTA)][Cl] (**4**) was synthesized.

Thus, heating concentrated toluene solutions of **1a** and PTA in a ratio 1:2.3 produced **2**, which precipitated from the reaction mixture and was isolated as a yellow solid in 85 % yield. When the same reaction was carried out using a stoichiometric amount of PTA and more diluted solutions in hot toluene, **3** was isolated as an air-stable yellow solid in 79 % yield (Scheme 2). Moreover, **3** reacts with an excess of PTA, giving rise to **2** (Scheme 2). The corresponding complexes with Tpms coordinated in a κ^3(*N,N,O*) fashion could not be synthesized as fast isomerization from **1b** to

1a occurs under the reaction conditions. In the same way, treatment of the analogous complex [RuCl{κ^3(*N,N,N*)-Tpm}(PPh$_3$)$_2$]Cl[13] with one equivalent of PTA in hot toluene led to **4** as a yellow air-stable solid in 79 % yield (Scheme 2).
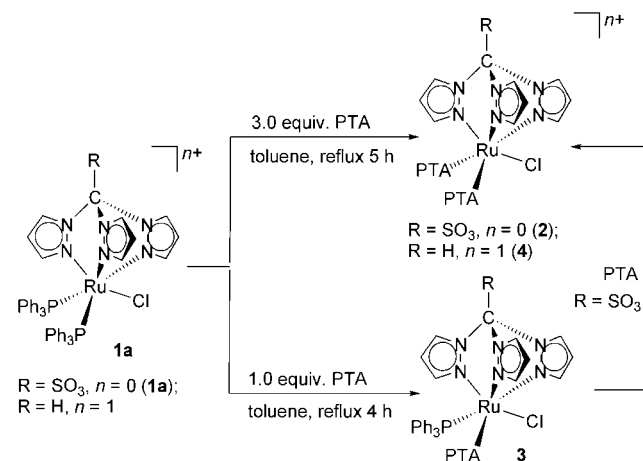
Scheme 2.

Complexes **2**, **3**, and **4** are soluble in common organic solvents such as methanol, chloroform, and dichloromethane and insoluble in diethyl ether and hexane. In spite of the presence of the sulfonate group and PTA unit, **3** is insoluble in water, and **2** is only slightly soluble in water (1.8 mg mL^{-1}). Surprisingly, **4** shows higher water solubility (2.8 mg mL^{-1}) than **2** and **3**, even though Tpm is supposed to induce lower water solubility than Tpms. The molar conductivity in nitromethane for **4** (76 S cm^2 mol^{-1}) agrees with a 1:1 electrolyte.[14] The complexes have been analytically and spectroscopically characterized (IR and ^{1}H, ^{13}C{^{1}H}, and ^{31}P{^{1}H} NMR spectroscopy). In particular, it should be noted that: (i) the IR spectra (KBr) show the characteristic ν(C–S) absorption for Tpms at 621 (**2**) and 622 cm^{-1} (**3**), (ii) the ^{31}P{^{1}H} spectrum exhibits a singlet at –33.1 ppm for **2** and two doublet resonances at 43.5 and –37.9 ppm ($J_{P,P}$ = 34 Hz) and 44.9 and –35.1 ppm ($J_{P,P}$ = 36 Hz) for the PPh$_3$ and the PTA ligands of **3** and **4**, respectively, (iii) the ^{1}H NMR spectrum of **2** in CDCl$_3$ shows the signals for the hydrogen atoms of the pyrazole rings *trans* to the phosphanes as two doublets at 9.05 and 8.07 ppm (3-H and 5-H) and a triplet at 6.45 ppm (4-H), and the hydrogen atoms for the ring *trans* to the chloride as two doublets at 9.24 and 7.19 ppm (3-H and 5-H) and a triplet at 6.43 ppm (4-H). For **3** the hydrogen atoms of the pyrazole rings are inequivalent and appear as doublets and triplets in the range 9.10–5.88. The ^{1}H NMR spectra also show the signals for the PTA ligands as AB spin systems of the NCH$_2$N group at 4.60 and 4.48 ppm ($J_{HA,HB}$ = 13 Hz) for **2** and at 4.45 and 4.26 ppm ($J_{HA,HB}$ = 13 Hz) for **3**. The NCH$_2$P protons appear as a singlet at 4.18 ppm in **2** and 3.91 ppm in **3**, (iv) ^{13}C{^{1}H} NMR spectra reveal the CH$_2$ groups of the PTA ligand as doublets at 73.3 ($^3J_{C,P}$ = 6 Hz) (NCH$_2$N) and 53.3 ppm ($J_{C,P}$ = 15 Hz) (NCH$_2$P) for **2** and at 73.2 ($^3J_{C,P}$ = 6 Hz) (NCH$_2$N) and 51.6 ppm ($J_{C,P}$ = 14 Hz)

S. Miguel, J. Diez, M. P. Gamasa, M. E. Lastra

(NCH$_2$P) for **3**. For both complexes, the signals for the pyrazole rings appear in the range 148.2–106.6 ppm, and (iv) ^{1}H NMR spectra are especially informative for Tpm complexes due to the methane Tpm proton, which appears at low field (12.24 ppm for **4**) separated from the rest of the proton resonances of the pyrazole rings in the range 8.87–5.86 ppm and those for the PTA phosphane, which appears as AB spin systems at 4.45 and 4.26 ppm (NCH$_2$N) and 3.96 and 3.89 ppm (NCH$_2$P). The signals in the ^{13}C{^{1}H} NMR spectra have been fully assigned and agree with the proposed complexes (see Exp. Sect.).

Slow evaporation of a water solution of **2**, and slow diffusion of hexane into an acetone solution of **3** resulted in crystals of **2**·4H$_2$O and **3**·2C$_3$H$_6$O suitable for X-ray diffrac-
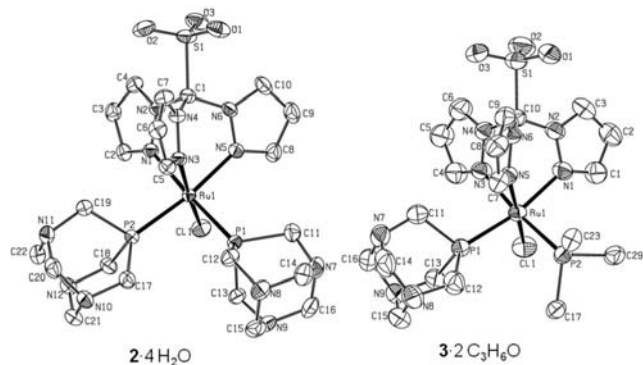

Figure 3. Molecular structure and atom labeling scheme for **2**·4H$_2$O and **3**·2C$_3$H$_6$O. Solvent molecules and hydrogen atoms have been omitted for clarity. Non-hydrogen atoms are represented by 50% probability ellipsoids.

Table 2. Selected bond lengths [Å] and angles [°] for **2**·CH$_2$Cl$_2$ and **3**·2C$_3$H$_6$O.

Selected bond lengths for **2**·CH$_2$Cl$_2$			
Ru(1)–N(1)	2.1252(14)	Ru(1)–P(1)	2.2937(4)
Ru(1)–N(3)	2.0639(14)	Ru(1)–P(2)	2.2859(4)
Ru(1)–N(5)	2.1248(14)	Ru(1)–Cl(1)	2.4105(4)
Selected bond angles for **2**·CH$_2$Cl$_2$			
N(1)–Ru(1)–N(3)	84.26(6)	N(5)–Ru(1)–P(2)	171.68(4)
N(1)–Ru(1)–N(5)	81.06(6)	N(1)–Ru(1)–Cl(1)	88.69(4)
N(3)–Ru(1)–N(5)	84.89(6)	N(3)–Ru(1)–Cl(1)	171.21(4)
N(1)–Ru(1)–P(1)	175.48(4)	N(5)–Ru(1)–Cl(1)	88.83(4)
N(1)–Ru(1)–P(2)	90.65(4)	P(1)–Ru(1)–Cl(1)	89.073(16)
N(3)–Ru(1)–P(1)	97.59(4)	P(2)–Ru(1)–Cl(1)	91.665(16)
N(3)–Ru(1)–P(2)	93.66(4)	P(1)–Ru(1)–P(2)	93.337(16)
N(5)–Ru(1)–P(1)	94.97(4)		
Selected bond lengths for **3**·2C$_3$H$_6$O			
Ru(1)–N(1)	2.145(3)	Ru(1)–P(1)	2.2971(8)
Ru(1)–N(3)	2.129(3)	Ru(1)–P(2)	2.3242(9)
Ru(1)–N(5)	2.071 (3)	Ru(1)–Cl(1)	2.4155(9)
Selected bond angles for **3**·2C$_3$H$_6$O			
N(1)–Ru(1)–N(3)	80.01(11)	N(5)–Ru(1)–P(2)	95.57(8)
N(1)–Ru(1)–N(5)	86.04(12)	N(1)–Ru(1)–Cl(1)	90.16(8)
N(3)–Ru(1)–N(5)	84.63(11)	N(3)–Ru(1)–Cl(1)	87.93(10)
N(1)–Ru(1)–P(1)	168.73(8)	N(5)–Ru(1)–Cl(1)	86.41(8)
N(1)–Ru(1)–P(2)	93.52(8)	P(1)–Ru(1)–Cl(1)	92.76(4)
N(3)–Ru(1)–P(1)	89.31(8)	P(2)–Ru(1)–Cl(1)	93.07(3)
N(3)–Ru(1)–P(2)	173.50(8)	P(1)–Ru(1)–P(2)	97.18(3)
N(5)–Ru(1)–P(1)	89.43(9)		

tion studies. ORTEP representations are shown in Figure 3, and selected bond lengths and angles are presented in Table 2.
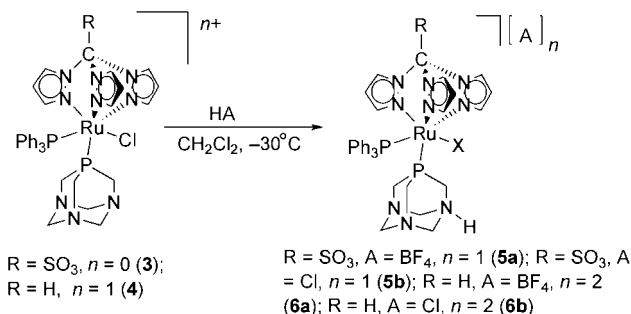
For both complexes, the ruthenium ion exhibits a distorted octahedral coordination geometry bonded to one chlorine atom, two phosphorus atoms of the phosphane ligands, and the nitrogen atoms of Tpms. The N–Ru–N angles and Ru–N bond lengths for both complexes are in the range found for hydridotris(pyrazolyl)borate ruthenium(II) complexes,[9] and the small N–Ru–N angles (80.01–86.04°) reflect the *fac* environment of the ligand around the ruthenium ion. The P–Ru–P angle in **3** [97.18(3)°] is significantly larger than that in **2** [93.337(16)°] as a consequence of the steric bulk of the PPh$_3$ ligand.

Electrophilic Attack on PTA Complexes

As we have reported previously,[15] complexes containing PTA ligands undergo electrophilic attack at the coordinated PTA yielding new complexes containing modified PTA phosphanes. Thus, **1a** reacts with different electrophiles to yield N-substituted derivatives.

Synthesis of [RuCl{κ^3(*N,N,N*)-Tpms}(PPh$_3$)(1-H-PTA)][X] [X = BF$_4$ (5a), Cl (5b)] and [RuCl{κ^3(*N,N,N*)-Tpm}(PPh$_3$)-(1-H-PTA)][X]$_2$ [X = BF$_4$ (6a), Cl (6b)]

Addition of an equimolecular amount of HBF$_4$ to a solution of **3** in dichloromethane at –30 °C produced [RuCl{κ^3(*N,N,N*)-Tpms}(PPh$_3$)(1-H-PTA)][BF$_4$] (**5a**), which precipitated upon addition of diethyl ether. In the same way, addition at –30 °C of an equimolecular amount of HBF$_4$ to a solution of [RuCl{κ^3(*N,N,N*)-Tpm}-(PPh$_3$)(PTA)][BF$_4$], generated in situ from **4** and NaBF$_4$, allows the isolation of [RuCl{κ^3(*N,N,N*)-Tpm}(PPh$_3$)(1-H-PTA)][BF$_4$]$_2$ (**6a**) as a yellow solid in 80% yield. The formation of **5a** and **6a** comes from the protonation of one nitrogen atom of the coordinated PTA ligand leading to the 3,5-diaza-1-azonia-7-phosphatricyclo[3.3.1.1^{3,7}]decane ligand (1-H-PTA, Scheme 3). Complexes [RuCl{κ^3(*N,N,N*)-Tpms}(PPh$_3$)(1-H-PTA)][Cl] (**5b**) and [RuCl{κ^3(*N,N,N*)-Tpm}(PPh$_3$)(1-H-PTA)][Cl]$_2$ (**6b**) were obtained by treatment of **3** and **4** in dichloromethane with a 2 N solution of HCl in diethyl ether at 0 °C. Elemental analyses and NMR

R = SO$_3$, n = 0 (**3**);
R = H, n = 1 (**4**)

R = SO$_3$, A = BF$_4$, n = 1 (**5a**); R = SO$_3$, A = Cl, n = 1 (**5b**); R = H, A = BF$_4$, n = 2 (**6a**); R = H, A = Cl, n = 2 (**6b**)

Scheme 3.

spectroscopic data support the proposed formulations. However, conductivity measurements in nitromethane indicate some differences since the conductivity values for **5b** (65 $Scm^2 mol^{-1}$) and **6b** (67 $Scm^2 mol^{-1}$) are significantly lower than expected for a 1:1 electrolyte (75–95 $Scm^2 mol^{-1}$) and 1:2 electrolyte (150–180 $Scm^2 mol^{-1}$),[14] whereas the values found for **5a** (83 $Scm^2 mol^{-1}$) and **6a** (182 $Scm^2 mol^{-1}$) agree with those expected. An explanation for the low values observed for **5b** and **6b** can be found in the formation of an ionic pair between the proton bonded to the nitrogen atom of the 1-H-PTA ligand and the chlorine counteranion. Unfortunately, this proton could not be identified in the ^1H NMR spectra of these complexes.

The relevant spectroscopic parameters for **5a** and **6a** are similar to those of **5b** and **6b** except for the $^{31}P\{^1H\}$ NMR spectra, which are quite different. Thus, the $^{31}P\{^1H\}$ spectra exhibit two doublets at 39.9 and –19.6 ppm ($^2J_{PP}$ = 34 Hz) for **5a** and 39.6 and –23.4 ppm ($^2J_{PP}$ = 33 Hz) for **5b** for PPh_3 and 1-H-PTA, respectively. In addition, the signals corresponding to the 1-H-PTA ligand for **6a** and **6b** are quite different: –24.2 ppm ($^2J_{PP}$ = 34 Hz) for **6a** and –20.7 ppm ($^2J_{PP}$ = 34 Hz) for **6b**. In all cases, the signal for the 1-H-PTA is clearly shifted to a lower field compared to the value found in **3** (–37.9 ppm) as previously reported for N-protonated PTA.[15] The differences in the chemical shift could be due to a weak hydrogen bonding interaction with the chlorine anion in **5b** and **6b**, which would agree with the low conductivity values. For the rest of the spectroscopic data, only the data corresponding to **5a** and **6a** will be discussed. Thus, for **5a** the IR spectrum (KBr) shows the characteristic ν(C–S) absorption for Tpms at 622 cm^{-1} and the ν(B–F) absorption at 1031 cm^{-1}. The ^1H NMR spectrum shows the expected AB systems for the hydrogen atoms of the NCH_2N and NCH_2P groups of PTA at 4.67 and 4.49 ppm (J_{HAHB} = 12 Hz) for **5a**, 4.59 and 4.47 ppm (J_{HAHB} = 12 Hz) for **6a**, and 3.91 and 3.45 ppm (J_{HCHD} = 13 Hz) for **5a**, and 3.87 ppm for **6a**, respectively. The $^{13}C\{^1H\}$ NMR spectrum reveals the CH_2 groups of PTA as doublet signals at 71.5 ($^3J_{CP}$ = 6 Hz) (NCH_2N) and 48.1 ppm (J_{CP} = 14 Hz) (NCH_2P) for **5a** and two singlets at 71.3 (NCH_2N) and 49.1 ppm (NCH_2P) for **6a**. The signals for the carbon atoms of the pyrazole rings appear in the range 149.8–106.9 ppm. The signal for the apical CSO_3 carbon atom for **5a** appears at 90.6 ppm.

Slow evaporation of NCMe solutions of **5a** and **6b** gave crystals suitable for X-ray diffraction studies. ORTEP representations of the complex cations are shown in Figure 4, and selected bond lengths and angles are collected in Table 3.

In both complexes, the ruthenium ion exhibits a distorted octahedral coordination geometry bonded to one chlorine atom, two phosphorus atoms of the phosphane ligands, and the nitrogen atoms of κ^3(N,N,N)-Tpms for **5a** and Tpm for **6b**. The N–Ru–N angles and Ru–N bond lengths for both complexes are in the range found for hydridotris(pyrazolyl)-borato-ruthenium(II) complexes.[16] The small N–Ru–N angles, in the range 79.70–86.25°, reflect the *fac* environment of the ligand around the ruthenium ion. The Ru–N
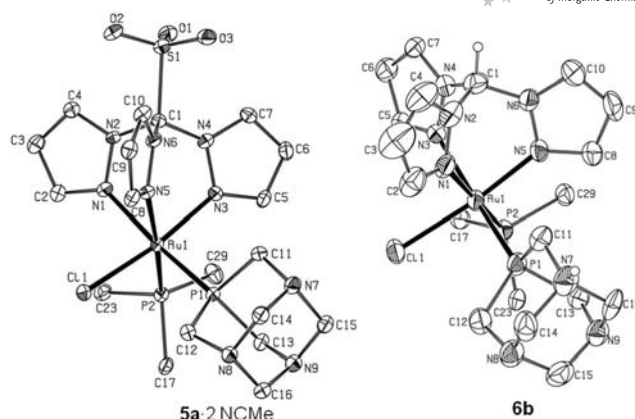

Figure 4. Molecular structure and atom labeling scheme for the complex cations of **5a·2NCMe** and **6b**. Solvent molecules and hydrogen atoms, except N–H, and the apical hydrogen atom of Tpm are omitted for clarity. Non-hydrogen atoms are represented by 50% probability ellipsoids.

Table 3. Selected bond lengths [Å] and angles [°] for **5a·2NCMe** and **6b**.

Selected bond lengths for 5a·2NCMe			
Ru(1)–N(1)	2.145(2)	Ru(1)–Cl(1)	2.4146(6)
Ru(1)–N(3)	2.071(2)	C(11)–N(7)	1.498(3)
Ru(1)–N(5)	2.120(2)	C(14)–N(7)	1.531(4)
Ru(1)–P(1)	2.2937(7)	C(15)–N(7)	1.527(3)
Ru(1)–P(2)	2.3199(6)	N(7)–H(1)	1.06(5)

Selected bond angles for 5a·2NCMe			
N(1)–Ru(1)–N(3)	86.25(9)	P(1)–Ru(1)–Cl(1)	91.23(2)
N(1)–Ru(1)–N(5)	79.70(9)	P(2)–Ru(1)–Cl(1)	92.44(2)
N(3)–Ru(1)–N(5)	83.80(8)	P(1)–Ru(1)–P(2)	96.13(2)

Selected bond lengths for 6b			
Ru(1)–N(1)	2.128(7)	Ru(1)–Cl(1)	2.409(2)
Ru(1)–N(3)	2.159(6)	C(11)–N(7)	1.505(11)
Ru(1)–N(5)	2.078(6)	C(14)–N(7)	1.570(12)
Ru(1)–P(1)	2.280(2)	C(16)–N(7)	1.511(12)
Ru(1)–P(2)	2.326(2)	N(7)–H(7N)	1.06(5)
H(7N)–Cl(3)	2.10	N(7)H–Cl	2.9769

| Selected bond angles for 6b			
N(1)–Ru(1)–N(3)	81.4(3)	P(1)–Ru(1)–Cl(1)	91.60(7)
N(1)–Ru(1)–N(5)	84.8(3)	P(2)–Ru(1)–Cl(1)	93.75(8)
N(3)–Ru(1)–N(5)	86.6(2)	P(1)–Ru(1)–P(2)	97.04(8)
N(7)–H(7N)–Cl(3)	171		

bond lengths *trans* to the phosphane ligands [2.145(2) and 2.120(2) Å] are significantly longer those *trans* to the chlorine atom [Ru(1)–N(3) = 2.071(2) Å], which is in accordance with the higher *trans* influence for the phosphane ligands.[12]

The most important feature for these complexes is the hydrogen bonding between the NH and the Cl⁻ counteranion found in **6b** (Figure 5). This N–H–Cl interaction can be demonstrated by the short H···Cl (2.10 Å) and N···Cl (2.9769 Å) distances as well as by the N–H–Cl angle (171°) close to 180°.[17] This interaction explains the low conductivity values obtained for **6b** compared with the high values obtained for **6a**, which has a BF_4^- counteranion.
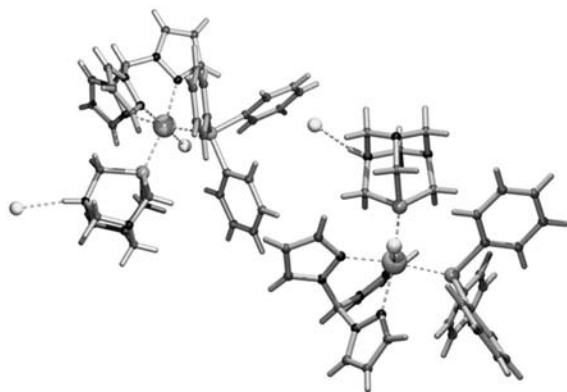
Figure 5. Hydrogen bonding in **6b**.

Synthesis of [RuCl{κ³(*N,N,N*)-Tpms}(PPh₃)(1-BH₃-PTA)] (7)

Complex **3** reacts with stoichiometric amounts of BH₃·THF in THF at room temperature to yield [RuCl-{κ³(*N,N,N*)-Tpms}(PPh₃)(1-BH₃-PTA)][BF₄] (**7**), which precipitated upon addition of hexane (Scheme 4).
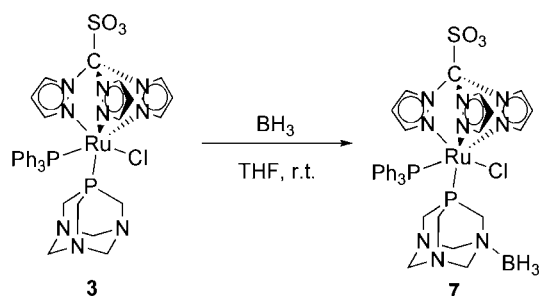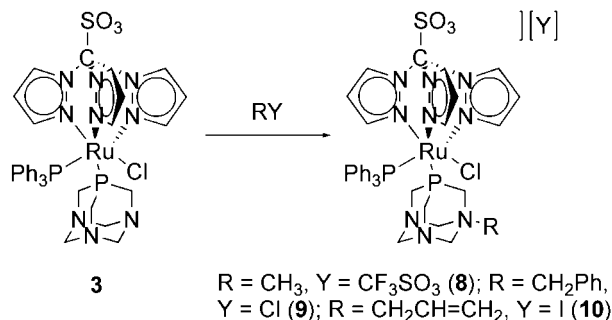

Scheme 4.

Complex **7** was isolated in 83% yield as a yellow air-stable solid and the spectroscopic data agree with the proposed stoichiometry. The more remarkable features are as follows: (i) the IR spectrum shows the characteristic absorptions for Tpms coordinated in the κ³(*N,N,N*) mode [1282, 1055 ν(S–O), 833 ν(C–N), and 622 ν(C–S) cm⁻¹]. The ν(B–H) absorptions are observed at 2370, 2292, and 2225 cm⁻¹, and the ν(N–B) absorption at 1170 cm⁻¹, (ii) the ³¹P{¹H} NMR spectrum shows two doublets at 40.8 and –27.8 ppm ($^2J_{PP}$ = 34 Hz) for the PPh₃ and the 1-BH₃-PTA ligands, respectively, (iii) the ¹¹B{¹H} NMR spectrum shows the signal for the BH₃ group at –10.40 ppm, and (iv) the ¹H and the ¹³C{¹H} NMR spectra have been fully assigned through COSY HH, HSQC, and HMBC experiments and agree with the proposed complexes.

PTA Alkylation Reactions. Synthesis of [RuCl{κ³(*N,N,N*)-Tpms}(PPh₃)(1-R-PTA)][Y] [R = CH₃, Y = CF₃SO₃ (8); R = CH₂Ph, Y = Cl (9); R = CH₂CH=CH₂, Y = I (10)]

The reaction of **3** with methyl triflate or organic halides such as benzyl chloride or allyl iodide in dichloromethane at room temperature led to [RuCl{κ³(*N,N,N*)-Tp}(PPh₃)(1-

R-PTA)][Y] [R = CH₃, Y = CF₃SO₃ (**8**); R = CH₂Ph, Y = Cl (**9**); R = CH₂CH=CH₂, Y = I (**10**)], which contain modified PTA ligands (Scheme 5). The complexes were isolated in 64–74% yield. The molar conductivities in acetonitrile (96–147 S cm² mol⁻¹) are in the range found for 1:1 electrolytes.

Scheme 5.

The spectroscopic data agree with the proposed stoichiometries. The more remarkable features are as follows: (i) the IR spectra show characteristic absorptions for the κ³(*N,N,N*) coordination mode of Tpms in **8**–**10**, (ii) the ³¹P{¹H} NMR spectra show two doublets in the range 39.1 to 39.8 ppm for PPh₃ and –12.2 to –15.8 ppm for 1-R-PTA ($^2J_{PP}$ = 33 Hz). The chemical shift of the modified PTA ligand, again clearly shifted to lower fields, agrees with the N-alkylation of the PTA ligand, and (iii) the ¹H NMR and ¹³C{¹H} NMR spectra have been fully assigned through COSY HH, HSQC, and HMBC NMR experiments and agree with the proposed complexes (see Exp. Sect.).

Conclusions

New ruthenium(II) scorpionate complexes have been synthesized and the coordination modes have been determined by X-ray diffraction. For complexes with Tpms, the thermodynamic product **1a** shows κ³(*N,N,N*) coordination of the ligand. The kinetic product, **1b**, which has κ³(*N,N,O*)-Tpms coordination, was also isolated.

PPh₃ substitution with PTA led to new complexes, which exhibit very low water solubility. Surprisingly, the complexes with Tpm show higher water solubility than those with Tpms. Electrophilic attacks on coordinated PTA gave rise to new PTA-substituted ruthenium(II) derivatives.

For **5b** and **6b**, hydrogen bonding interactions were established between the NH proton and chlorine anions. This interaction has been confirmed in **6b** by X-ray analysis.

Experimental Section

spectra were recorded with a Perkin–Elmer FT-IR Paragon 1000 spectrometer. Conductivities were measured at room temperature in ca. 5×10^{-4} mol dm^{-3} solutions, with a crison EC-Meter BASIC 30+ conductimeter. The C, H, and N analyses were carried out with a Perkin–Elmer 240-B microanalyzer. NMR spectra were recorded with Bruker AV400 and NAV400 instruments at 400.1 MHz (^{1}H), 100.6 MHz (^{13}C), 162.1 (^{31}P), and 128.4 (^{11}B) and Bruker AV300 and 300DPX instruments at 300.1 MHz (^{1}H) and 121.5 MHz (^{31}P), using SiMe$_4$ or 85% H$_3$PO$_4$ as standards. DEPT experiments were carried out for all the compounds. Coupling constants J are given in Hertz. Resonances due to the Tpm and Tpms ligands are reported by chemical shift and multiplicity only, as all $^3J_{\text{H,H}}$ values for the pyrazolyl rings are 2 Hz. Abbreviations used: br, broad signal; d, doublet; t, triplet; dd, double doublet; m, multiplet; sept, septuplet; s, singlet.

[RuCl{κ^3(*N,N,N*)-Tpms}(PPh$_3$)$_2$] (1a): To a solution of [RuCl$_2$(PPh$_3$)$_3$] (120 mg, 0.13 mmol) in methanol (15 mL) was added LiTpms (39 mg, 0.13 mmol). The reaction mixture was heated to reflux for 4 h before the volatiles were removed in vacuo. The solid residue was extracted into CH$_2$Cl$_2$, filtered through kieselguhr, and concentrated under vacuum to a volume of approx. 1 mL. Addition of hexane afforded a yellow precipitate. The solvents were decanted, and the solid residue was washed with hexane (3 × 30 mL) and dried under reduced pressure to afford **1a**. Yield: 118 mg (95%). C$_{47}$H$_{41}$Cl$_3$N$_6$O$_3$P$_2$RuS (1038.1): calcd. C 54.32, H 3.98, N 8.09, S 3.09; found C 54.18, H 3.73, N 7.65, S 2.61. IR (KBr pellet): $\tilde{\nu}$ = 1286 [ν(S–O)], 1054, 832 [ν(C–N)], 622 [ν(C–S)] cm^{-1}. ^{1}H NMR (400.5 MHz, CDCl$_3$, 20 °C): δ = 9.10 [d, 1 H, 3-H and 5-H (pz)], 8.91 [d, 2 H, 3-H and 5-H (pz)], 7.29–7.09 (m, 30 H, PPh$_3$), 6.99 [d, 2 H, 3-H and 5-H (pz)], 5.85 [t, 2 H, 4-H (pz)], 5.42 [t, 1 H, 4-H (pz)], 5.21 [d, 1 H, 3-H and 5-H (pz)] ppm. ^{13}C{^{1}H} NMR (100.6 MHz, CDCl$_3$, 20 °C): δ = 149.8 [s, C-3 and C-5 (pz)], 147.1 [s, C-3 and C-5 (pz)], 137.5 [s, C-3 and C-5 (pz)], 136.9 [s, C-3 and C-5 (pz)], 134.3 (s, C-2, C-6 and C-3, C-5 PPh$_3$), 132.7 (d, $J_{\text{C,P}}$ = 38 Hz, C-1 PPh$_3$), 129.6 (s, C-4 PPh$_3$), 128.0 (C-2, C-6 and C-3, C-5 PPh$_3$), 106.5 [s, C-4 (pz)], 105.7 [s, C-4 (pz)], 90.8 (s, *C*SO$_3$) ppm. ^{31}P{^{1}H} NMR (121.5 MHz, CDCl$_3$, 20 °C): δ = 38.9 (s, PPh$_3$) ppm.

[RuCl{κ^3(*N,N,O*)-Tpms}(PPh$_3$)$_2$] (1b): A solution of LiTpms (156 mg, 0.52 mmol) in methanol (5 mL) was added to a solution of [RuCl$_2$(PPh$_3$)$_3$] (500 mg, 0.52 mmol) in CH$_2$Cl$_2$ (50 mL) at 0 °C. The mixture was stirred for 20 min and then evaporated to dryness. The residue was extracted into CH$_2$Cl$_2$ and concentrated under vacuum to a volume of approx. 1 mL. Addition of hexane afforded an orange precipitate. The solvents were decanted, and the solid residue was washed with hexane (3 × 30 mL) and dried under reduced pressure to afford **1b**. Yield: 283 mg (57%). IR (KBr pellet): $\tilde{\nu}$ = 1088, 860 [ν(C–N)], 621 [ν(C–S)] cm^{-1}. ^{1}H NMR (400.5 MHz, CDCl$_3$, 20 °C): 9.00 [d, 1 H, 3-H and 5-H (pz)], 7.90 [d, 1 H, 3-H and 5-H (pz)], 7.40–7.00 (m, 30 H, PPh$_3$), 6.99 [d, 2 H, 3-H and 5-H (pz)], 6.97 [d, 2 H, 3-H and 5-H (pz)], 6.60 [t, 1 H, 4-H (pz)], 5.79 [t, 2 H, 4-H (pz)] ppm. ^{13}C{^{1}H} NMR (100.6 MHz, CDCl$_3$, –20 °C): 148.6 [s, C-3 and C-5 (pz)], 142.9 [s, C-3 and C-5 (pz)], 136.6 [s, C-3 and C-5 (pz)], 135.4 [s, C-3 and C-5 (pz)], 135.1 (s, C-2, C-6 and C-3, C-5 PPh$_3$), 134.3 (s, C-1 PPh$_3$), 129.1 (s, C-4 PPh$_3$), 127.4 (s, C-2, C-6 and C-3, C-5 PPh$_3$), 108.3 [s, C-4 (pz)], 106.4 [s, C-4 (pz)], 94.7 (s, *C*SO$_3$) ppm. ^{31}P{^{1}H} NMR (162.1 MHz, CDCl$_3$, 20 °C): 35.8 (s, PPh$_3$) ppm.

[RuCl{κ^3(*N,N,N*)-Tpms}(PTA)$_2$] (2): To a solution of **1a** (100 mg, 0.105 mmol) in toluene (12 mL) was added PTA (38 mg, 0.241 mmol). The reaction mixture was heated to reflux for 6 h, and a yellow precipitate formed. The solid was collected by fil-

tration, washed with hexane, and dried under vacuum to give **3**. Yield: 66 mg (85%). C$_{25}$H$_{40}$ClN$_{12}$O$_3$P$_2$RuS (787.1): calcd. C 38.14, H 5.12, N 21.35, S 4.07; found C 37.75, H 4.93, N 20.14, S 3.88. IR (KBr pellet): $\tilde{\nu}$ = 1278, 1053 [ν(S–O)], 813 [ν(C–N)], 622 [ν(C–S)] cm^{-1}. ^{1}H NMR (400.5 MHz, CDCl$_3$, 20 °C): 9.24 [d, 1 H, 3-H and 5-H (pz)], 9.05 [d, 2 H, 3-H and 5-H (pz)], 8.07 [d, 2 H, 3-H and 5-H (pz)], 7.19 [d, 1 H, 3-H and 5-H (pz)], 6.45 [t, 2 H, 4-H (pz)], 6.43 [t, 1 H, 4-H (pz)], 4.60 (AB spin system, 6 H, J_{HAHB} = 13 Hz, NC*H*$_2$N), 4.48 (AB spin system, 6 H, J_{HAHB} = 13 Hz, NC*H*$_2$N), 4.18 (s, 12 H, NC*H*$_2$P) ppm. ^{13}C{^{1}H} NMR (100.6 MHz, CDCl$_3$, 20 °C): 148.2 [s, C-3 and C-5 (pz)], 145.3 [s, C-3 and C-5 (pz)], 138.5 [s, C-3 and C-5 (pz)], 137.1 [s, C-3 and C-5 (pz)], 107.5 [s, C-4 (pz)], 107.1 [s, C-4 (pz)], 90.8 (s, *C*-SO$_3$), 73.3 (d, $^3J_{\text{CP}}$ = 6 Hz, NC*H*$_2$N), 53.3 (d, J_{CP} = 15 Hz, NC*H*$_2$P) ppm. ^{31}P{^{1}H} NMR (162.1 MHz, CDCl$_3$, 20 °C): –33.1 (s, PTA) ppm.

[RuCl{κ^3(*N,N,N*)-Tpms}(PPh$_3$)(PTA)] (3): To a solution of **1a** (145 mg, 0.15 mmol) in toluene (80 mL) was added PTA (28 mg, 0.15 mmol). The reaction mixture was heated to reflux for 4.5 h. The solvent was evaporated under vacuum and the yellow solid obtained was recrystallized from CH$_2$Cl$_2$/hexane. Yield: 100 mg (79%). C$_{34}$H$_{36}$ClN$_9$O$_3$P$_2$RuS (849.1): calcd. C 48.09, H 4.27, N 14.84, S 3.78; found C 48.72, H 4.50, N 14.98, S 3.57. IR (KBr pellet): $\tilde{\nu}$ = 1285, 1054 [ν(S–O)], 834 [ν(C–N)], 621 [ν(C–S)] cm^{-1}. ^{1}H NMR (400.5 MHz, CDCl$_3$, 20 °C): δ = 9.10 [d, 1 H, 3-H and 5-H (pz)], 9.04 [d, 1 H, 3-H and 5-H (pz)], 9.0 [d, 1 H, 3-H and 5-H (pz)], 8.33 [d, 1 H, 3-H and 5-H (pz)], 7.61–7.34 (m, 15 H, PPh$_3$), 6.77 [d, 1 H, 3-H and 5-H (pz)], 6.47 [t, 1 H, 4-H (pz)], 5.98 [t, 1 H, 4-H (pz)], 5.88 [m, 2 H, 3-H, 5-H, and 4-H (pz)], 4.45 (AB spin system, J_{HAHB} = 13 Hz, 3 H, NC*H*$_2$N), 4.26 (AB spin system, J_{HAHB} = 13 Hz, 3 H, NC*H*$_2$N), 3.91 (s, 6 H, NC*H*$_2$P) ppm. ^{13}C{^{1}H} NMR (100.6 MHz, CDCl$_3$, 20 °C): δ = 147.8 [s, C-3 and C-5 (pz)], 145.8 [s, C-3 and C-5 (pz)], 145.3 [s, C-3 and C-5 (pz)], 137.7 [s, C-3 and C-5 (pz)], 137.1 [s, C-3 and C-5 (pz)], 136.9 [s, C-3 and C-5 (pz)] 133.8 (d, $^2J_{\text{CP}}$ = 9 Hz, C-2 and C-6 PPh$_3$), 130.1 (s, C-4 PPh$_3$), 128.5 (d, $^2J_{\text{CP}}$ = 9 Hz, C-3 and C-5 PPh$_3$), 107.2 [s, C-4 (pz)], 106.8 [s, C-4 (pz)], 106.6 [s, C-4 (pz)], 90.6 (s, *C*SO$_3$), 73.2 (d, $^3J_{\text{CP}}$ = 6 Hz, NC*H*$_2$N), 51.6 (d, J_{CP} = 14 Hz, NC*H*$_2$P) ppm. ^{31}P{^{1}H} NMR (161.9 MHz, CDCl$_3$, 20 °C): δ = 43.5 (d, $^2J_{\text{PP}}$ = 34 Hz, PPh$_3$), –37.9 (d, $^2J_{\text{PP}}$ = 34 Hz, PTA) ppm.

[RuCl{κ^3(*N,N,N*)-Tpm}(PPh$_3$)(PTA)][Cl] (4): To a solution of complex [RuCl{κ^3(*N,N,N*)-Tpm}(PPh$_3$)$_2$][Cl] (100 mg, 0.110 mmol) in toluene (15 mL) was added PTA (17 mg, 0.110 mmol). The reaction mixture was heated to reflux for 5 h. The solvent was evaporated under vacuum, and the yellow solid obtained was recrystallized from CH$_2$Cl$_2$/hexane. Yield: 70 mg (79%). $S_{20\,°C}$ (H$_2$O) = 2.8 mg mL^{-1}. C$_{34}$H$_{37}$Cl$_2$N$_9$P$_2$Ru (805.1): calcd. C 50.69, H 4.63, N 15.61; found C 50.67, H 4.94, N 15.61. Molar conductivity in nitromethane: Λ_M = 76 S cm^2 mol^{-1}. ^{1}H NMR (400.5 MHz, CD$_2$Cl$_2$, 20 °C): 12.24 (s, 1 H, H$_{\text{apical}}$), 8.87 [d, 1 H, 3-H and 5-H (pz)], 8.81 [d, 1 H, 3-H and 5-H (pz)], 8.74 [d, 1 H, 3-H and 5-H (pz)], 8.28 [d, 1 H, 3-H and 5-H (pz)], 7.71–7.37 (m, 15 H, PPh$_3$), 6.74 [d, 1 H, 3-H and 5-H (pz)], 6.50 [d, 1 H, 4-H (pz)], 6.08 [d, 1 H, 4-H (pz)], 5.97 [d, 1 H, 4-H (pz)], 5.86 [d, 1 H, 3-H and 5-H (pz)], 4.45 (AB spin system, 3 H, J_{HAHB} = 14 Hz, NC*H*$_2$N), 4.26 (AB spin system, 3 H, J_{HAHB} = 14 Hz, NC*H*$_2$N), 3.96 (CD spin system, 3 H, J_{HCHD} = 15 Hz, NC*H*$_2$P), 3.89 (CD spin system, 3 H, J_{HCHD} = 15 Hz, NC*H*$_2$P) ppm. ^{13}C{^{1}H} NMR (100.6 MHz, CD$_2$Cl$_2$, 20 °C): 148.0 [s, C-3 and C-5 (pz)], 146.2 [s, C-3 and C-5 (pz)], 145.4 [s, C-3 and C-5 (pz)], 134.6 [s, C-3 and C-5 (pz)], 134.3 [s, C-3 and C-5 (pz)], 133.7 (d, $^2J_{\text{CP}}$ = 9 Hz, C-2 and C-6 PPh$_3$), 130.1 (s, C-4 PPh$_3$), 128.5 (d, $^2J_{\text{CP}}$ = 9 Hz, C-3 and C-5 PPh$_3$), 108.1 [s, C-4 (pz)], 107.9 [s, C-4 (pz)], 107.6 [s, C-4 (pz)], 73.2 (s, *C*H), 73.1 (d, $^3J_{\text{CP}}$ = 6 Hz, NC*H*$_2$N), 51.9 (d, J_{CP} = 15 Hz, NC*H*$_2$P) ppm. ^{31}P{^{1}H} NMR

(161.9 MHz, CDCl$_3$, 20 °C): 44.9 (d, $^2J_{PP}$ = 36 Hz, PPh$_3$), –35.1 (d, $^2J_{PP}$ = 36 Hz, PTA) ppm.

[RuCl{κ^3(*N*,*N*,*N*)-Tpms}(PPh$_3$)(1-H-PTA)][BF$_4$] (5a): To a solution of **3** (100 mg, 0.118 mmol) in CH$_2$Cl$_2$ (8 mL) at –30 °C was added a diethyl ether solution of HBF$_4$·OEt$_2$ (36 μL, 0.142 mmol). The reaction mixture was stirred at this temperature for 1.5 h. The yellow solution was filtered, and the filtrate was reduced under vacuum to about 1 mL. Addition of diethyl ether afforded a yellow precipitate. The solvents were decanted, and the solid residue was washed with diethyl ether and dried under vacuum. Yield: 88 mg (79%). C$_{36}$H$_{41}$BCl$_3$F$_4$N$_9$O$_3$P$_2$RuS (1105.1): calcd. C 39.06, H 3.73, N 11.39, S 2.90; found C 38.28, H 4.49, N 11.46, S 3.19. Molar conductivity in nitromethane: Λ_M = 83 S cm^2 mol^{-1}. IR (KBr pellet): ṽ = 1296 [ν(S–O)], 835 [ν(C–N)], 622 [ν(C–S)], 1031 [ν(B–F)] cm^{-1}. ^{1}H NMR (300.13 MHz, CD$_3$CN, 20 °C): δ = 9.01 [d, 1 H, 3-H and 5-H (pz)], 8.98 [d, 2 H, 3-H and 5-H (pz)], 8.32 [d, 1 H, 3-H and 5-H (pz)], 7.51–7.41 (m, 15 H, PPh$_3$), 6.87 [d, 1 H, 3-H and 5-H (pz)], 6.58 [d, 1 H, 4-H (pz)], 6.46 [d, 1 H, 3-H and 5-H (pz)], 6.13 [d, 1 H, 4-H (pz)], 6.05 [d, 1 H, 4-H (pz)], 4.67 (AB spin system, J_{HAHB} = 12 Hz, 3 H, NC*H*$_2$N), 4.49 (AB spin system, J_{HAHB} = 12 Hz, 3 H, NC*H*$_2$N), 3.91 (CD spin system, J_{HCHD} = 13 Hz, 3 H, NC*H*$_2$P), 3.45 (CD spin system, J_{HCHD} = 13 Hz, 3 H, NC*H*$_2$P) ppm. ^{13}C{^{1}H} NMR (100.6 MHz, CD$_3$CN, 20 °C): δ = 149.8 [s, C-3 and C-5 (pz)], 146.4 [s, C-3 and C-5 (pz)], 145.9 [s, C-3 and C-5 (pz)], 137.4 [s, C-3 and C-5 (pz)], 137.0 [s, C-3 and C-5 (pz)], 136.9 [s, C-3 and C-5 (pz)], 133.7 (d, $^2J_{CP}$ = 9 Hz, C-2 and C-6, PPh$_3$), 133.2 (s, C-1 PPh$_3$), 130.5 (s, C-4, PPh$_3$), 128.8 (d, $^2J_{CP}$ = 9 Hz, C-3 and C-5, PPh$_3$), 107.8 [s, C-4 (pz)], 107.6 [s, C-4 (pz)], 106.9 [s, C-4 (pz)], 90.6 (s, *C*SO$_3$), 71.5 (d, $^3J_{CP}$ = 6 Hz, NC*H*$_2$N, PTA), 48.1 (d, J_{CP} = 14 Hz, NC*H*$_2$P, PTA) ppm. ^{31}P{^{1}H} NMR (121.5 MHz, CD$_3$CN, 20 °C): δ = 39.9 (d, $^2J_{PP}$ = 34 Hz, PPh$_3$), –19.6 (d, $^2J_{PP}$ = 34 Hz, PTA) ppm.

[RuCl{κ^3(*N*,*N*,*N*)-Tpms}(PPh$_3$)(1-H-PTA)][Cl] (5b): To a solution of **3** (100 mg, 0.118 mmol) in CH$_2$Cl$_2$ (6 mL) at 0 °C was added a 2 N HCl·OEt$_2$ solution (71 μL, 0.142 mmol). The reaction mixture was stirred at this temperature for 2.5 h. The addition of hexane (50 mL) afforded a yellow precipitate. The solvents were decanted, and the solid residue was washed with hexane (2 × 30 mL) and dried under vacuum. Yield: 89 mg (86%). C$_{40}$H$_{51}$Cl$_2$N$_9$O$_3$P$_2$RuS (971.1): calcd. C 49.43, H 5.29, N 12.97, S 3.30; found C 49.30, H 5.39, N 13.09, S 3.59. Molar conductivity in nitromethane: Λ_M = 65 S cm^2 mol^{-1}. IR (KBr pellet): ṽ = 1282, 1055 [ν(S–O)], 835 [ν(C–N)], 622 [ν(C–S)] cm^{-1}. ^{1}H NMR (400.1 MHz, CD$_2$Cl$_2$, 20 °C): 9.09 [d, 1 H, 3-H and 5-H (pz)], 9.01 [d, 2 H, 3-H and 5-H (pz)], 8.31 [d, 1 H, 3-H and 5-H (pz)], 7.55–7.40 (m, 15 H, PPh$_3$), 6.85 [d, 1 H, 3-H and 5-H (pz)], 6.52 [d, 1 H, 4-H (pz)], 6.23 [d, 1 H, 3-H and 5-H (pz)], 6.07 [d, 1 H, 4-H (pz)], 6.02 [d, 1 H, 4-H (pz)], 4.64–4.44 (broad signal, 6 H, NC*H*$_2$N), 4.02–3.89 (broad signal, 6 H, NC*H*$_2$P) ppm. ^{13}C{^{1}H} NMR (100.6 MHz, CD$_3$CN, 20 °C): 148.6 [s, C-3 and C-5 (pz)], 146.0 [s, C-3 and C-5 (pz)], 137.6 [s, C-3 and C-5 (pz)], 137.1 [s, C-3 and C-5 (pz)], 133.6 (d, C-2 and C-6, $^2J_{CP}$ = 9 Hz, PPh$_3$), 133.1 (s, C-1, PPh$_3$), 130.5 (s, C-4, PPh$_3$), 128.7 (d, C-3 and C-5, $^2J_{CP}$ = 9 Hz, PPh$_3$), 107.5 [s, C-4 (pz)], 106.6 [s, C-4 (pz)], 90.6 (s, *C*SO$_3$), 71.6 (s, NC*H*$_2$N), 49.3 (broad s, NC*H*$_2$P) ppm. ^{31}P{^{1}H} NMR (121.5 MHz, CD$_2$Cl$_2$, 20 °C): 39.6 (d, $^2J_{PP}$ = 33 Hz, PPh$_3$), –23.4 (d, $^2J_{PP}$ = 33 Hz, PTA) ppm.

[RuCl{κ^3(*N*,*N*,*N*)-Tpm}(PPh$_3$)(1-H-PTA)][BF$_4$]$_2$ (6a): Complex **4** (100 mg, 0.124 mmol) was dissolved in CH$_2$Cl$_2$ (10 mL), and the yellow solution was cooled to –30 °C and stirred for 15 min. NaBF$_4$ (136 mg, 1.24 mmol) and HBF$_4$·OEt$_2$ (22 μL, 0.149 mmol) were added. The mixture was stirred at this temperature for 1.5 h. The solution was filtered through kieselghur, and the filtrate was re-

duced under vacuum to about 1 mL. The addition of hexane afforded a yellow precipitate. The solvent was decanted, and the solid residue was washed with hexane and dried under vacuum. Yield: 94 mg (80%). C$_{35}$H$_{40}$B$_2$Cl$_3$F$_8$N$_9$P$_2$Ru (1042.1): calcd. C 40.82, H 3.92, N 12.24; found C 40.3, H 4.76, N 13.63. Molar conductivity in nitromethane: Λ_M = 182 S cm^2 mol^{-1}. ^{1}H NMR (300.13 MHz, [D$_6$]DMSO, 20 °C): δ = 9.91 (s, 1 H, H$_{apical}$), 8.48 [m, 3 H, 3-H and 5-H (pz)], 8.42 [d, 1 H, 3-H and 5-H (pz)], 7.47–7.40 (m, 15 H, PPh$_3$), 6.67 [d, 1 H, 3-H and 5-H (pz)], 6.64 [d, 1 H, 3-H and 5-H (pz)], 6.59 [d, 1 H, 4-H (pz)], 6.36 [d, 1 H, 4-H (pz)], 6.15 [d, 1 H, 4-H (pz)], 4.59 (AB spin system, J_{HAHB} = 12 Hz, 3 H, NC*H*$_2$N), 4.47 (AB spin system, J_{HAHB} = 12 Hz, 3 H, NC*H*$_2$N), 3.87 (s, 6 H, NC*H*$_2$P) ppm. ^{13}C{^{1}H} NMR (75.46 MHz, [D$_6$]-DMSO, 20 °C): δ = 150.9 [s, C-3 and C-5 (pz)], 147.8 [s, C-3 and C-5 (pz)], 146.4 [s, C-3 and C-5 (pz)], 136.7 [s, C-3 and C-5 (pz)], 135.5 [s, C-3 and C-5 (pz)], 134.5 [s, C-3 and C-5 (pz)], 133.2 (s, C-2 and C-6, PPh$_3$), 130.9 (s, C-4, PPh$_3$), 129.2 (s, C-3 and C-5, PPh$_3$), 111.2 [s, C-4 (pz)], 109.3 [s, C-4 (pz)], 108.1 [s, C-4 (pz)], 75.3 (s, *C*SO$_3$), 71.3 (s, NC*H*$_2$N, PTA), 49.1 (s, NC*H*$_2$P, PTA) ppm. ^{31}P{^{1}H} NMR (162.1 MHz, [D$_6$]DMSO, 20 °C): δ = 43.0 (d, $^2J_{PP}$ = 34 Hz, PPh$_3$), –24.2 (broad signal, PTA) ppm.

[RuCl{κ^3(*N*,*N*,*N*)-Tpm}(PPh$_3$)(1-H-PTA)][Cl]$_2$ (6b): To a solution of **4** (100 mg, 0.124 mmol) in CH$_2$Cl$_2$ (7 mL) at 0 °C was added a 2 N HCl·OEt$_2$ solution (74 μL, 0.148 mmol). The reaction mixture was stirred at this temperature for 1.5 h. The addition of hexane (50 mL) afforded a yellow precipitate. The solvents were decanted, and the solid residue was washed with hexane and dried under vacuum. Yield: 74 mg (71%). C$_{34}$H$_{37}$Cl$_3$N$_9$P$_2$Ru (841.1): calcd. C 48.55, H 4.43, N 12.65; found C 48.31, H 4.12, N 13.07. Molar conductivity in nitromethane: Λ_M = 67 S cm^2 mol^{-1}. ^{1}H NMR (300.1 MHz, CDCl$_3$, 20 °C): 12.53 (s, 1 H, H apical), 8.98 [d, 1 H, 3-H and 5-H (pz)], 8.85 [d, 2 H, 3-H and 5-H (pz)], 8.26 [d, 1 H, 3-H and 5-H (pz)], 7.42–7.29 (m, 15 H, PPh$_3$), 6.74 [d, 1 H, 3-H and 5-H (pz)], 6.49 [d, 1 H, 4-H (pz)], 6.38 [d, 1 H, 3-H and 5-H (pz)], 6.09 [d, 2 H, 4-H (pz)], 4.62 (AB spin system, J_{HAHB} = 13 Hz, 3 H, NC*H*$_2$N), 4.49 (AB spin system, J_{HAHB} = 13 Hz, 3 H, NC*H*$_2$N), 4.05 (CD spin system, J_{HCHD} = 15 Hz, 3 H, NC*H*$_2$P), 3.85 (CD spin system, J_{HCHD} = 15 Hz, 3 H, NC*H*$_2$P) ppm. ^{13}C{^{1}H} NMR (100.6 MHz, CD$_3$CN, 20 °C): 149.3 [s, C-3 and C-5 (pz)], 145.7 [s, C-3 and C-5 (pz)], 137.3 [s, C-3 and C-5 (pz)], 136.8 [s, C-3 and C-5 (pz)], 133.1 (d, C-2 and C-6, $^2J_{CP}$ = 9 Hz, PPh$_3$), 132.8 (s, C-1 PPh$_3$), 130.5 (s, C-4, PPh$_3$), 128.5 (d, C-3 and C-5, $^2J_{CP}$ = 9 Hz, PPh$_3$), 107.3 [s, C-4 (pz)], 105.9 [s, C-4 (pz)], 90.4 (s, *C*SO$_3$), 71.4 (S, NC*H*$_2$N, PTA), 48.9 (s, NC*H*$_2$P, PTA) ppm. ^{31}P{^{1}H} NMR (121.4 MHz, CDCl$_3$, 20 °C): 40.7 (d, $^2J_{PP}$ = 34 Hz, PPh$_3$), –20.7 (d, $^2J_{PP}$ = 34 Hz, PTA) ppm.

[RuCl{κ^3(*N*,*N*,*N*)-Tpms}(PPh$_3$)(1-BH$_3$-PTA)] (7): To a solution of **3** (50 mg, 0.059 mmol) in tetrahydrofuran (5 mL) was added BH$_3$·THF (60 μL, 0.059 mmol), and the mixture was stirred for 1 h at room temperature. The addition of hexane (50 mL) afforded a yellow precipitate. The solvents were decanted, and the solid residue was washed with hexane and dried under vacuum. Yield: 42 mg (83%). C$_{34}$H$_{39}$BClN$_9$O$_3$P$_2$RuS (863.1): calcd. C 47.31, H 4.55, N 14.61, S 3.72; found C 46.88, H 4.39, N 14.40, S 3.60. IR (KBr pellet): ṽ = 1282, 1055 [ν(S–O)], 833 [ν(C–N)], 622 [ν(C–S)], 2370, 2292, 2225 [ν(B–H)], 1170 [ν(N–B)] cm^{-1}. ^{1}H NMR (400.1 MHz, CD$_2$Cl$_2$, 20 °C): δ = 9.1 [d, 1 H, 3-H and 5-H (pz)], 9.01 [d, 2 H, 3-H and 5-H (pz)], 8.26 [d, 1 H, 3-H and 5-H (pz)], 7.55–7.39 (m, 15 H, PPh$_3$), 6.86 [d, 1 H, 3-H and 5-H (pz)], 6.52 [d, 1 H, 4-H (pz)], 6.18 [d, 1 H, 3-H and 5-H (pz)], 6.06 [d, 1 H, 4-H (pz)], 6.01 [d, 1 H, 4-H (pz)], 4.20 (m, 6 H, NC*H*$_2$N), 3.70 (m, 6 H, NC*H*$_2$P), 1.19 (broad, 3 H, PTA–B*H*$_3$) ppm. ^{11}B{^{1}H} NMR (128.4 MHz, CD$_2$Cl$_2$, 20 °C): δ = –10.40 ppm. ^{13}C{^{1}H} NMR (100.6 MHz,

CD$_2$Cl$_2$, 20 °C): δ = 148.4 [s, C-3 and C-5 (pz)], 145.9 [s, C-3 and C-5 (pz)], 145.7 [s, C-3 and C-5 (pz)], 137.8 [s, C-3 and C-5 (pz)], 137.1 [s, C-3 and C-5 (pz)], 137.0 [s, C-3 and C-5 (pz)], 133.7 (d, C-2 and C-6, $^2J_{CP}$ = 9 Hz, PPh$_3$), 133.3 (s, C-1 PPh$_3$), 130.4 (s, C-4 PPh$_3$), 128.6 (d, C-3 and C-5, $^2J_{CP}$ = 9 Hz, PPh$_3$), 107.2 [s, C-4 (pz)], 107.1 [s, C-4 (pz)], 106.6, [s, C-4 (pz)], 90.6 (s, CSO$_3$), 77.6, (s, NCH$_2$N, PTA), 70.8, (d, NCH$_2$N, PTA), 67.7 (s, NCH$_2$N, PTA), 54.7 (d, J_{CP} = 15 Hz, NCH$_2$P, PTA), 48.9 (d, J_{CP} = 15 Hz, NCH$_2$P, PTA), 48.7 (d, J_{CP} = 15 Hz, NCH$_2$P, PTA) ppm. ^{31}P\{^{1}H\} NMR (162.1 MHz, CD$_2$Cl$_2$, 20 °C): δ = 40.8 (d, $^2J_{PP}$ = 34 Hz, PPh$_3$), –27.8 (d, $^2J_{PP}$ = 34 Hz, PTA) ppm.

[RuCl\{κ^3(*N*,*N*,*N*)-Tpms\}(PPh$_3$)(1-CH$_3$-PTA)][CF$_3$SO$_3$] (8): Complex **3** (100 mg, 0.118 mmol) was dissolved in CH$_2$Cl$_2$ (2 mL) at –30 °C. After 15 min, methyl trifluoromethanesulfonate (14 μL, 0.118 mmol) was added and the reaction mixture was stirred for 1 h at low temperature. Addition of hexane (50 mL) afforded a yellow precipitate. The solvents were decanted, and the solid residue was washed with hexane and dried under vacuum. Yield: 77 mg (65%). C$_{36}$H$_{39}$ClF$_3$N$_9$O$_6$P$_2$RuS$_2$ (1013.1): calcd. C 42.67, H 3.88, N 12.44, S 6.33; found C 41.91, H 4.00, N 12.01, S 5.81. Molar conductivity in acetonitrile: Λ_M = 147 S cm^2 mol^{-1}. IR (KBr pellet): $\tilde{\nu}$ = 1278, 1030 [ν(S–O)], 835 [ν(C–N)], 623 [ν(C–S)] cm^{-1}. ^{1}H NMR (300.1 MHz, CD$_3$CN, 20 °C): 9.05 [d, 1 H, 3-H and 5-H (pz)], 9.01 [d, 1 H, 3-H and 5-H (pz)], 8.99 [d, 1 H, 3-H and 5-H (pz)], 8.33 [d, 1 H, 3-H and 5-H (pz)], 7.55–7.40 (m, 15 H, PPh$_3$), 6.88 [d, 1 H, 3-H and 5-H (pz)], 6.73 [d, 1 H, 3-H and 5-H (pz)], 6.57 [t, 1 H, 4-H (pz)], 6.16 [t, 1 H, 4-H (pz)], 6.11 [t, 1 H, 4-H (pz)], 4.74–4.56 (m, 2 H, CH$_3$NCH_2N), 4.29–4.24 (m, 4 H, NCH_2N), 4.17–3.92 (m, 2 H, CH$_3$NCH_2P), 3.86–3.30 (m, 4 H, NCH_2P), 2.62 (s, 3 H, NCH_3) ppm. ^{13}C\{^{1}H\} NMR (100.6 MHz, CD$_3$CN, 20 °C): 150.3 [s, C-3 and C-5 (pz)], 146.7 [s, C-3 and C-5 (pz)], 145.9 [s, C-3 and C-5 (pz)], 137.5 [s, C-3 and C-5 (pz)], 137.1 [s, C-3 and C-5 (pz)], 137.0 [s, C-3 and C-5 (pz)], 133.8 (d, C-2 and C-6, $^2J_{CP}$ = 9 Hz, PPh$_3$), 133.2 (s, C-1, PPh$_3$), 130.6 (s, C-4, PPh$_3$) 128.7 (d, C-3 and C-5, $^3J_{CP}$ = 9 Hz, PPh$_3$), 117.3 (q, J_{CF} = 314 Hz, CF$_3$SO$_3$), 107.8 [s, C-4 (pz)], 107.5 [s, C-4 (pz)], 107.0 [s, C-4 (pz)], 90.7 (s, CSO$_3$), 80.5 (s, CH$_3$NCH_2N), 68.8 (d, $^3J_{CP}$ = 5 Hz, NCH_2N), 56.3 (d, J_{CP} = 9 Hz, CH$_3$NCH_2P), 49.3 (s, NCH$_3$), 47.2 (d, J_{CP} = 15 Hz, NCH$_2$P) ppm. ^{31}P\{^{1}H\} NMR (121.5 MHz, CD$_3$CN, 20 °C): 39.1 (d, $^2J_{PP}$ = 33 Hz, PPh$_3$), –15.8 (d, $^2J_{PP}$ = 33 Hz, PTA) ppm.

[RuCl\{κ^3(*N*,*N*,*N*)-Tpms\}(PPh$_3$)(1-CH$_2$=CHCH$_2$-PTA)][I] (9): Allyl iodide (22 μL, 0.24 mmol) was added to a solution of **3** (100 mg, 0.12 mmol) in CH$_2$Cl$_2$ (8 mL). The reaction mixture was stirred at room temperature for 2 h. The addition of hexane (50 mL) afforded **9** as a yellow solid. The solvents were decanted, and the solid residue was washed with hexane and dried under reduced pressure. Yield: 101 mg (83%). C$_{38}$H$_{43}$Cl$_3$IN$_9$O$_3$P$_2$RuS (1101.0): calcd. C 41.41, H 3.93, N 11.44, S 2.91; found C 41.48, H 4.62, N 11.20, S 3.13. Molar conductivity in acetonitrile: Λ_M = 96 S cm^2 mol^{-1}. IR (KBr pellet): $\tilde{\nu}$ = 1281, 1054 [ν(S–O)], 856 [ν(C–N)], 621 [ν(C–S)], 1623 [ν(C=C)] cm^{-1}. ^{1}H NMR (400.1 MHz, [D$_6$]DMSO, 20 °C): δ = 8.95 [d, 1 H, 3-H and 5-H (pz)], 8.92 [d, 1 H, 3-H and 5-H (pz)], 8.88 [d, 1 H, 3-H and 5-H (pz)], 8.43 [d, 1 H, 3-H and 5-H (pz)], 7.53–7.41 (m, 15 H, PPh$_3$), 7.10 [d, 1 H, 3-H and 5-H (pz)], 6.70 [d, 1 H, 4-H (pz)], 6.68 [d, 1 H, 3-H and 5-H (pz)], 6.34 [d, 1 H, 4-H (pz)], 6.24 [d, 1 H, 4-H (pz)], 5.82–5.76 (m, 1 H, NCH$_2$CH=CH$_2$), 5.63–5.59 (m, 2 H, NCH$_2$CH=CH_2), 4.94–4.88 (m, 2 H, NCH_2NCH$_2$CH=CH$_2$), 4.77–4.69 (m, 2 H, NCH_2NCH$_2$CH=CH$_2$), 4.33–4.15 (m, 4 H, NCH_2N), 4.09–4.05 (m, 2 H, PCH_2NCH$_2$CH=CH$_2$), 3.85–3.77 (m, 4 H, NCH_2P), 3.65 (d, 2 H, NCH$_2$CH=CH$_2$) ppm. ^{13}C\{^{1}H\} NMR (100.7 MHz, [D$_6$]-DMSO, 20 °C): δ = 151.5 [s, C-3 and C-5 (pz)], 147.7 [s, C-3 and C-5 (pz)], 145.8 [s, C-3 and C-5 (pz)], 137.6 [s, C-3 and C-5 (pz)],

137.1 [s, C-3 and C-5 (pz)], 137.0 [s, C-3 and C-5 (pz)], 133.9 (d, C-2 and C-6 PPh$_3$), 133.4 (s, C-1 PPh$_3$), 131.0 (s, C-4 PPh$_3$), 129.2 (d, C-3 and C-5 PPh$_3$), 128.9 (s, NCH$_2$CH=CH$_2$), 124.1 (s, NCH$_2$CH=CH$_2$), 108.5 [s, C-4 (pz)], 107.8 [s, C-4 (pz)], 107.7 [s, C-4 (pz)], 90.6 (s, CSO$_3$), 79.2 (s, NCH_2NCH$_2$CH=CH$_2$), 77.9 (s, NCH_2NCH$_2$CH=CH$_2$), 72.3 (s, NCH$_2$N), 68.7 (s, NCH$_2$CH=CH$_2$), 50.8, (d, J_{CP} = 9 Hz, NCH_2P), 46.9 (d, J_{CP} = 9 Hz, PCH$_2$NCH$_2$CH=CH$_2$), 46.6 (d, J_{CP} = 9 Hz, NCH_2P) ppm. ^{31}P\{^{1}H\} NMR (162.1 MHz, [D$_6$]DMSO, 20 °C): δ = 39.8 (d, $^2J_{PP}$ = 33 Hz, PPh$_3$), –15.2 (d, $^2J_{PP}$ = 33 Hz, PTA) ppm.

[RuCl\{κ^3(*N*,*N*,*N*)-Tpms\}(PPh$_3$)(1-PhCH$_2$-PTA)][Cl] (10): Benzyl chloride (70 μL) was added to a solution **2** (100 mg, 0.12 mmol) in CH$_2$Cl$_2$ (5 mL). The reaction mixture was stirred for 24 h. The addition of hexane (50 mL) afforded **8**. The solvents were decanted, and the solid residue was washed with hexane and dried under reduced pressure. Yield: 90 mg (77%). C$_{42}$H$_{45}$Cl$_4$N$_9$O$_3$P$_2$RuS (1059.1): calcd. C 47.56, H 4.28, N 11.88, S 3.02; found C 48.19, H 4.96, N 11.65, S 3.26. Molar conductivity in acetonitrile: Λ_M = 119 S cm^2 mol^{-1}. IR (KBr pellet): $\tilde{\nu}$ = 1293, 1054 [ν(S–O)], 834 [ν(C–N)], 621 [ν(C–S)] cm^{-1}. ^{1}H NMR (300.1 MHz, CD$_3$CN, 20 °C): 8.98 [d, 2 H, 3-H and 5-H (pz)], 8.94 [d, 1 H, 3-H and 5-H (pz)], 8.52 [d, 1 H, 3-H and 5-H (pz)], 7.50–7.32 (m, 20 H, PPh$_3$ and Ph), 6.85 [d, 1 H, 3-H and 5-H (pz)], 6.61 [d, 1 H, 3-H and 5-H (pz)], 6.56 [d, 1 H, 4-H (pz)], 6.12 [d, 1 H, 4-H (pz)], 6.02 [d, 1 H, 4-H (pz)], 5.36–5.32 (m, 2 H, PhCH$_2$NCH_2N), 4.83–4.75 (m, 2 H, PhCH$_2$NCH_2N), 4.54–4.41 (m, 4 H, PhCH_2 and NCH_2N), 4.16–4.11 (m, 2 H, PhCH$_2$NCH_2P), 3.75–3.70 (m, 4 H, NCH_2P) ppm. ^{13}C\{^{1}H\} NMR (100.6 MHz, CD$_3$CN, 20 °C): 150.7 [s, C-3 and C-5 (pz)], 147.2 [s, C-3 and C-5 (pz)], 145.9 [s, C-3 and C-5 (pz)], 137.3 [s, C-3 and C-5 (pz)], 136.9 [s, C-3 and C-5 (pz)], 136.8 [s, C-3 and C-5 (pz)], 133.7–125.6 (Ph and PPh$_3$), 107.9 [s, C-4 (pz)], 107.6 [s, C-4 (pz)], 106.9 [s, C-4 (pz)], 90.6 (s, CSO$_3$), 79.3 (s, PhCH$_2$NCH_2N), 78.2 (s, PhCH$_2$NCH_2N), 68.9 (s, NCH_2N), 64.1 (s, PhCH$_2$N), 51.9 (d, J_{CP} = 15 Hz, PhCH$_2$NCH_2P), 47.0 (d, J_{CP} = 15 Hz, NCH_2P) ppm. ^{31}P\{^{1}H\} NMR (121.5 MHz, CD$_3$CN, 20 °C): 39.9 (d, $^2J_{PP}$ = 33 Hz, PPh$_3$), –12.2 (d, $^2J_{PP}$ = 33 Hz, PTA) ppm.

X-Ray Crystal Structure Determination of Complexes 1a, 1b, 2, 3, 5a, and 6b: Relevant crystal and refinement data are collected in Table 4 and Table 5.

Data collection was performed at 293(2) K with an Oxford Diffraction Xcalibur Nova single crystal diffractometer using Cu-K_α radiation (λ = 1.5418 Å) (**1a, 1b, 2, 5a,** and **6b**). Images were collected at a 65 mm fixed crystal-detector distance using the oscillation method, with 1° oscillation and variable exposure time per image 3–20, 20–100, 3–5, 20–70, and 20–130 s for **1a, 1b, 2, 5a,** and **6b**, respectively. Diffraction data for **3** were recorded with an Oxford Diffraction Gemini S single crystal diffractometer using Cu-K_α radiation (λ = 1.5418 Å) Images were collected at a 55 mm fixed crystal-detector distance using the oscillation method, with 1° oscillation and variable exposure time per image 5–50 s. In all cases the data collection strategy was calculated with the program CrysAlis Pro CCD.[21] Data reduction and cell refinement was performed with the program CrysAlis Pro RED.[21] An empirical absorption correction was applied using the SCALE3 ABSPACK algorithm as implemented in the program CrysAlis Pro RED.[21] The software package WINGX[22] was used for space group determination, structure solution, and refinement. The structures of the complexes were solved by Patterson interpretation and phase expansion using DIRDIF.[23] Isotropic least-squares refinement on F^2 using SHELXL97[24] was performed. During the final stages of refinement, all the positional parameters and the anisotropic temperature factors of all the non-H atoms were refined, except C atoms of the

Table 4. Crystal data and structure refinement for **1a**, **1b**, and **2**.

	1a·CH₂Cl₂	**1b·THF**	**2·4H₂O**
Chemical formula	$C_{47}H_{41}Cl_3N_6O_3P_2RuS$	$C_{50}H_{47}ClN_6O_4P_2RuS$	$C_{22}H_{41}ClN_{12}O_7P_2RuS$
fw	1039.28	1026.46	816.19
Crystal system	triclinic	monoclinic	triclinic
Space group	$P\bar{1}$	$P2_1/c$	$P\bar{1}$
a [Å]	12.3238(3)	17.7447(1)	11.0589(2)
b [Å]	13.1656(3)	14.3433(1)	12.2137(2)
c [Å]	16.0094(4)	18.0578(2)	13.4458(3)
α [°]	93.653(2)	90	97.540(2)
β [°]	95.020(2)	92.992(1)	97.944(2)
γ [°]	116.650(2)	90	115.980(2)
V [Å³]	2297.15(10)	4589.76(7)	1578.98(5)
Z	2	4	2
$\rho_{calcd.}$ [g cm⁻³]	1.503	1.485	1.717
μ [mm⁻¹]	5.847	4.815	6.926
$F(000)$	1060	2112	840
Crystal size [mm]	0.21 × 0.17 × 0.11	0.074 × 0.054 × 0.025	0.1 × 0.09 × 0.07
θ range [°]	3.78 to 64.34	3.94 to 66.84	3.40 to 73.88
Index ranges	–14 ≤ h ≤ 14	–21 ≤ h ≤ 21	–13 ≤ h ≤ 12
	–15 ≤ k ≤ 15	–13 ≤ k ≤ 17	–15 ≤ k ≤ 15
	–18 ≤ l ≤ 18	–16 ≤ l ≤ 21	–16 ≤ l ≤ 16
Reflections collected	32232	24408	32686
Unique reflections	7693 [R(int) = 0.0336]	8053 [R(int) = 0.0548]	6310 [R(int) = 0.0223]
Completeness to θ max. [%]	99.9	98.8	98.6
Parameters/restraints	568/0	561/7	447/8
Goodness-of-fit on F^2	1.059	0.819	1.066
R_1[a] [$I > 2\sigma(I)$]; wR_2[a] [$I > 2\sigma(I)$]	0.0381; 0.1074	0.0392; 0.0861	0.0207; 0.0529
$R1$(all data); $wR2$(all data)	0.0689; 0.0907	0.0410; 0.1092	0.0219; 0.0558
Largest diff. peak and hole [e Å⁻³]	1.168 and –1.299	1.151 and –0.625	0.302 and –0.526

[a] $R_1 = \Sigma(|F_o| - |F_c|)/\Sigma|F_o|$; $wR_2 = \{\Sigma[w(F_o^2 - F_c^2)^2]/\Sigma[w(F_o^2)^2]\}^{1/2}$.

Table 5. Crystal data and structure refinement for **3**, **5a**, and **6b**.

	3·2C₃H₆O	**5a·2 NCMe**	**6b**
Chemical formula	$C_{37}H_{42}ClN_9O_4P_2RuS$	$C_{38}H_{43}BClF_4N_{11}O_3P_2RuS$	$C_{35}H_{40}Cl_5N_9P_2Ru$
fw	907.32	1019.16	927.02
Crystal system	monoclinic	monoclinic	orthorhombic
Space group	$P2_1/c$	$P2_1/c$	$Pbca$
a [Å]	17.8466(3)	19.0825(3)	19.1872(4)
b [Å]	10.0996(2)	10.1250(2)	16.2722(3)
c [Å]	22.7777(4)	21.9137(3)	25.2421(8)
α [°]	90	90	90
β [°]	104.394(2)	97.5300(10)	90
γ [°]	90	90	90
V [Å³]	3976.66(12)	4197.44(12)	7881.0(3)
Z	4	4	8
$\rho_{calcd.}$ [g cm⁻³]	1.515	1.613	1.563
μ [mm⁻¹]	5.492	5.409	7.429
$F(000)$	1864	2080	3776
Crystal size [mm]	0.102 × 0.061 × 0.02	0.091 × 0.075 × 0.034	0.155 × 0.052 × 0.022
θ range [°]	4.01 to 70.66	4.07 to 74.30	3.97 to 61.49
Index ranges	–21 ≤ h ≤ 21	–22 ≤ h ≤ 23	–21 ≤ h ≤ 15
	–10 ≤ k ≤ 12	–12 ≤ k ≤ 8	–18 ≤ k ≤ 15
	–27 ≤ l ≤ 16	–27 ≤ l ≤ 25	–28 ≤ l ≤ 28
Reflections collected	14982	16214	23311
Unique reflections	7423 [R(int) = 0.0479]	8205 [R(int) = 0.0257]	6004 [R(int) = 0.0891]
Completeness to θ max. [%]	97.3	95.9	98.0
Parameters/restraints	498/0	731/0	477/1
Goodness-of-fit on F^2	0.840	1.127	0.834
R_1[a] [$I > 2\sigma(I)$]; wR_2[a] [$I > 2\sigma(I)$]	0.0357; 0.0743	0.0336; 0.0944	0.0585; 0.1392
$R1$(all data); $wR2$(all data)	0.0649; 0.0809	0.0376; 0.1051	0.1242; 0.1550
Largest diff. peak and hole [e Å⁻³]	0.402 and –0.717	0.714 and –1.349	0.919 and –0.761

[a] $R_1 = \Sigma(|F_o| - |F_c|)/\Sigma|F_o|$; $wR_2 = \{\Sigma[w(F_o^2 - F_c^2)^2]/\Sigma[w(F_o^2)^2]\}^{1/2}$.

C_4H_8 solvent molecule for **1b** (these disordered atoms were located by difference maps and isotropically refined). The H atoms were geometrically located and their coordinates were refined riding on their parent atoms, except hydrogen atoms of water molecules in **2**,

hydrogen atoms in **5a**, and H7n and H1 in **6b** (the coordinates of these H atoms were found from different Fourier maps and included in a refinement with isotropic parameters). The minimized function was $[(\Sigma w F_o^2 - F_c^2)/\Sigma w(F_o^2)]^{1/2}$ where $w = 1/[\sigma^2(F_o^2) + (aP)^2 + bP]$ (a and b values are collected in Table 3) with $\sigma(F_o2)$ from counting statistics and $P = [\text{Max} (F_o^2, 0) + 2F_c^2]/3$. Atomic scattering factors were taken from the International Tables for X-ray Crystallography.[25] Geometrical calculations were made with PARST.[26] The crystallographic plots were made with PLATON[27] and ORTEP-3 for Windows.[28]

CCDC-830526 (for **1a**), -830527 (for **1b**), -830528 (for **2**), -830529 (for **3**), -830530 (for **5a**), and -830531 (for **6b**) contain the supplementary crystallographic data for this paper. These data can be obtained free of charge from The Cambridge Crystallographic Data Centre via www.ccdc.cam.ac.uk/data_request/cif.

Acknowledgments

[1] a) C. Pettinari, C Santini, in: *Comprehensive Coordination Chemistry II* (Eds.: J. A. McCleverty, T. J. Meyer), Elsevier, **2003**, vol. 1, pp. 159–210; b) S. Trofimenko, *Scorpionates, The Coordination Chemistry of Polypyrazolylborate Ligands*, Imperial College Press, **1999**; c) C. Slugovc, I. Padilla-Martinez, S. Sirol, E. Carmona, *Coord. Chem. Rev.* **2001**, *213*, 129–157; d) M. D. Ward, J. A. McCleverty, J. C. Jeffery, *Coord. Chem. Rev.* **2001**, *222*, 251–272; e) D. L. Reger, *Coord. Chem. Rev.* **1996**, *147*, 571–595.

[2] C. Pettinari, R. Pettinari, *Coord. Chem. Rev.* **2005**, *249*, 525–543.

[3] W. Kläui, M. Berghahn, G. Rheinwald, H. Lang, *Angew. Chem.* **2000**, *112*, 2590; *Angew. Chem. Int. Ed.* **2000**, *39*, 2464–2466.

[4] a) D. V. Fomitchev, C. C. McLauchlan, R. H. Holm, *Inorg. Chem.* **2002**, *41*, 958–966; b) R. S. Herrick, T. J. Brunker, C. Maus, K. Crandall, A. Cetin, C. J. Ziegler, *Chem. Commun.* **2006**, 4330–4331; c) E. C. B. Alegria, L. M. D. R. S. Martins, M. Haukka, A. J. L. Pombeiro, *Dalton Trans.* **2006**, 4954–4961.

[5] a) C. Dinoi, M. F. Guedes da Silva, C. B. A. Elisabete, P. Smolenski, L. M. D. R. S. Martins, R. Poli, A. J. L. Pombeiro, *Eur. J. Inorg. Chem.* **2010**, 2415–2424; b) C. C. McLauchlan, M. P. Weberski, B. A. Greiner, *Inorg. Chim. Acta* **2009**, *362*, 2662–2666; c) C. Santini, M. Pellei, G. Lobbia, G. Gioia, A. Cingolani, R. Spagna, M. Camalli, *Inorg. Chem. Commun.* **2002**, *5*, 430–433.

[6] E. T. Papish, M. T. Taylor, F. E. Jernigan III, M. J. Rodig, R. R. Shawhan, G. P. A. Yap, F. A. Jove, *Inorg. Chem.* **2006**, *45*, 2242–2250.

[7] a) W. Kläui, D. Schramm, W. Peters, *Eur. J. Inorg. Chem.* **2001**, 3113–3117; b) W. Kläui, D. Schramm, W. Peters, G. Rheinwald, H. Lang, *Eur. J. Inorg. Chem.* **2001**, 1415–1424; c) P. Smolenski, C. Dinoi, M. F. C. Guedes da Silva, A. J. L. Pombeiro, *J. Organomet. Chem.* **2008**, *693*, 2338–2344.

[8] C. M. Nagaraja, M. Nethaji, B. R. Jagirdar, *Organometallics* **2007**, *26*, 6307–6311.

[9] a) A. García-Fernandez, J. Díez, A. Manteca, J. Sánchez, M. P. Gamasa, E. Lastra, *Polyhedron* **2008**, *27*, 1214–1228; b) A. García-Fernandez, J. Díez, A. Manteca, J. Sanchez, R. García-Nava, B. G. Sierra, F. Mollinedo, M. P. Gamasa, E. Lastra, *Dalton Trans.* **2010**, *39*, 10186–10196.

[10] T. B. Chenskaya, M. Berghahn, P. C. Kunz, W. Frank, W. Kläui, *J. Mol. Struct.* **2007**, *829*, 135–148.

[11] a) R. Wanke, P. Smolenski, M. F. C. Guedes da Silva, L. M. D. R. S. Martins, A. J. L. Pombeiro, *Inorg. Chem.* **2008**, *47*, 10158–10168; b) W. Kläui, M. Berghahn, W. Frank, G. J. Reiß, T. Schönherr, G. Rheinwald, H. Lang, *Eur. J. Inorg. Chem.* **2003**, 2059–2070.

[12] a) S. Pavlik, K. Mereiter, M. Puchberger, K. Kirchner, *J. Organomet. Chem.* **2005**, *690*, 5497–5507, and references cited therein; b) M. Jiménez-Tenorio, M. D. Palacios, M. C. Puerta, P. Valerga, *Organometallics* **2005**, *24*, 3088–3098, and references cited therein; c) T. G. Appleton, H. C. Clark, L. E. Manzer, *Coord. Chem. Rev.* **1973**, *10*, 335–422.

[13] L. D. Field, B. A. Messerle, L. Soler, I. E. Buys, T. W. Hambley, *J. Chem. Soc., Dalton Trans.* **2001**, 1959–1965.

[14] W. J. Geary, *Coord. Chem. Rev.* **1971**, *7*, 81–122.

[15] A. García-Fernandez, J. Díez, M. P. Gamasa, E. Lastra, *Inorg. Chem.* **2009**, *48*, 2471–2481.

[16] B. Buriez, I. D. Burns, A. F. Hill, A. J. P. White, D. J. Williams, J. D. E. T. Wilton-Ely, *Organometallics* **1999**, *18*, 1504–1516.

[17] a) T. Steiner, *Angew. Chem.* **2002**, *114*, 50; *Angew. Chem. Int. Ed.* **2002**, *41*, 48–76; b) T. Steiner, *Cryst. Rev.* **1996**, 1–57; c) G. A. Jeffrey, H. Maluszynska, J. Mitra, *Int. J. Biol. Macromol.* **1985**, *7*, 336–348.

[18] T. A. Stephenson, G. Wilkinson, *J. Inorg. Nucl. Chem.* **1966**, *28*, 945–956.

[19] D. L. Reger, T. C. Grattan, K. J. Brown, C. A. Little, J. J. S. Lamba, A. L. Rheingold, R. D. Sommer, *J. Organomet. Chem.* **2000**, *607*, 120–131.

[20] D. J. Daigle, *Inorg. Synth.* **1998**, *32*, 40–45.

[21] *CrysAlisPro CCD, CrysAlisPro RED*, Oxford Diffraction Ltd., Abingdon, Oxfordshire, UK, **2008**.

[22] L. J. Farrugia, *J. Appl. Crystallogr.* **1999**, *32*, 837.

[23] P. T. Beurskens, G. Beurskens, R. de Gelder, J. M. M. Smits, S. García-Granda, R. O. Gould, C. Smykalla, *The DIRDIF Program System*, Technical Report of the Crystallographic Laboratory, University of Nijmegen, The Netherlands, **2008**.

[24] G. M. Sheldrick, *SHELXL97: Program for the Refinement of Crystal Structures*; University of Göttingen, Germany, **2008**.

[25] *International Tables for X-ray Crystallography*, Kynoch Press, Birminghan, U. K., **1974**, vol. IV (present distributor: Kluwer Academic Publishers, Dordrecht, The Netherlands).

[26] M. Nardelli, *Comput. Chem.* **1983**, *7*, 95–98.

[27] A. L. Spek, *PLATON: A Multipurpose Crystallographic Tool*, University of Utrecht, The Netherlands, **2005**.

[28] ORTEP-3 for Windows®: L. J. Farrugia, *J. Appl. Crystallogr.* **1997**, *30*, 565.